LSD1 Controls Timely MyoD Expression via MyoD Core Enhancer Transcription

Isabella Scionti, Shinichiro Hayashi, Sandrine Mouradian, Emmanuelle Girard, Joana Esteves de Lima, Véronique Morel, Thomas Simonet, Maud Wurmser, Pascal Maire, Katia Ancelin, et al.

Article

Cell Reports

LSD1 Controls Timely *MyoD* Expression via MyoD Core Enhancer Transcription

Graphical Abstract

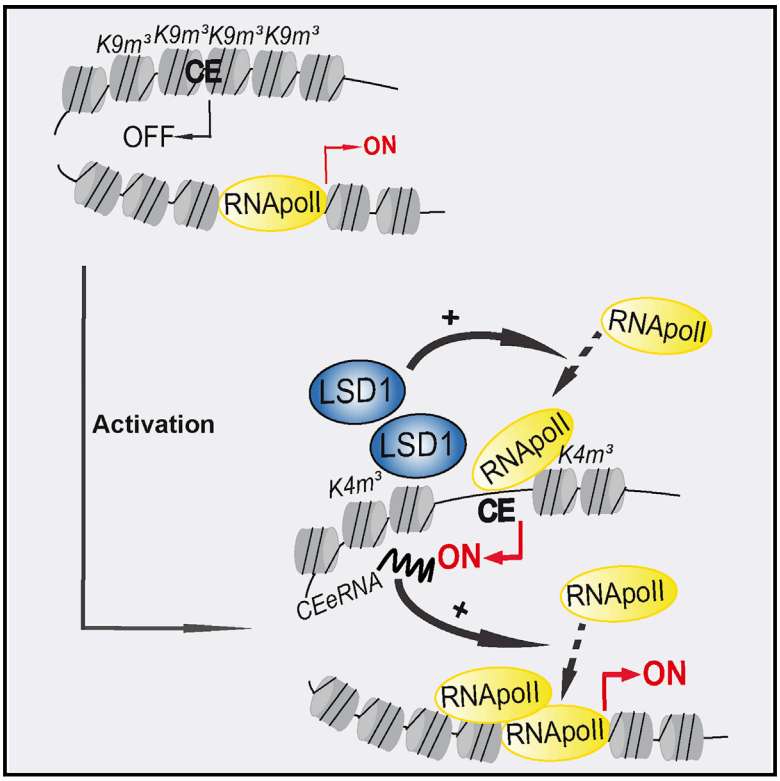

Highlights

- LSD1 participates in enhancer function by promoting eRNA transcription
- LSD1 contributes to activate *MyoD* during commitment of muscle cells
- LSD1 is recruited on the MyoD core enhancer (CE) during muscle differentiation
- LSD1 activates the transcription of the *MyoD* core enhancer eRNA

Authors

Isabella Scionti, Shinichiro Hayashi, Sandrine Mouradian, ..., Evelyne Goillot, Frederic Relaix, Laurent Schaeffer

Correspondence

evelyne.goillot@ens-lyon.fr (E.G.), laurent.schaeffer@univ-lyon1.fr (L.S.)

In Brief

Scionti et al. show that LSD1 is recruited on the MyoD core enhancer, where it promotes the transcription of an enhancer RNA that controls the timing of MyoD expression during myoblast commitment. This provides the first evidence that LSD1 is required for the transcription of enhancer RNAs from a pro-differentiation enhancer.

Scionti et al., 2017, Cell Reports *18*, 1996–2006
February 21, 2017
http://dx.doi.org/10.1016/j.celrep.2017.01.078

CellPress

OPEN ACCESS
CellPress

Cell Reports
Article

LSD1 Controls Timely *MyoD* Expression via MyoD Core Enhancer Transcription

Isabella Scionti,[1,2] Shinichiro Hayashi,[3,4] Sandrine Mouradian,[1,2] Emmanuelle Girard,[1,2,9] Joana Esteves de Lima,[3] Véronique Morel,[1,2] Thomas Simonet,[1,2] Maud Wurmser,[5] Pascal Maire,[5] Katia Ancelin,[1] Eric Metzger,[6,7,8] Roland Schüle,[6,7,8] Evelyne Goillot,[1,2,*] Frederic Relaix,[3] and Laurent Schaeffer[1,2,9,10,*]

[1]Institut NeuroMyoGene, CNRS UMR5310, INSERM U1217, Université Lyon1, 46 Allée d'Italie, 69007 Lyon, France
[2]Laboratory of Molecular Biology of the Cell, CNRS UMR5239, Université Lyon 1, ENS Lyon, 46 Allée d'Italie, 69007 Lyon, France
[3]Biology of the Neuromuscular System, INSERM IMRB-E10 U955, Université Paris-Est, 8 rue du Général Sarrail, 94010 Créteil Cedex, France
[4]Department of Cellular and Molecular Medicine, Medical Research Institute, Tokyo Medical and Dental University, 1-5-45 Yushima, Bunkyo-ku, Tokyo 113-8510, Japan
[5]Institut Cochin, INSERM U1016, CNRS UMR 8104, Université Paris Descartes, Sorbonne Paris Cité, 22 rue Mechain, 75014 Paris, France
[6]Klinik für Urologie und Zentrale Klinische Forschung, Klinikum der Universität Freiburg, Breisacherstrasse 66, 79106 Freiburg, Germany
[7]Deutsches Konsortium für Translationale Krebsforschung, Standort Freiburg, 79106 Freiburg, Germany
[8]BIOSS Centre of Biological Signalling Studies, Albert Ludwigs University Freiburg, 79106 Freiburg, Germany
[9]Hospices Civils de Lyon, Faculté de Medicine Lyon Est, 3 Quai des Célestins, 69002 Lyon, France
[10]Lead Contact
*Correspondence: evelyne.goillot@ens-lyon.fr (E.G.), laurent.schaeffer@univ-lyon1.fr (L.S.)
http://dx.doi.org/10.1016/j.celrep.2017.01.078

SUMMARY

MyoD **is a master regulator of myogenesis. Chromatin modifications required to trigger *MyoD* expression are still poorly described. Here, we demonstrate that the histone demethylase LSD1/KDM1a is recruited on the *MyoD* core enhancer upon muscle differentiation. Depletion of *Lsd1* in myoblasts precludes the removal of H3K9 methylation and the recruitment of RNA polymerase II on the core enhancer, thereby preventing transcription of the non-coding enhancer RNA required for *MyoD* expression (CEeRNA). Consistently, *Lsd1* conditional inactivation in muscle progenitor cells during embryogenesis prevented transcription of the CEeRNA and delayed *MyoD* expression. Our results demonstrate that LSD1 is required for the timely expression of *MyoD* in limb buds and identify a new biological function for LSD1 by showing that it can activate RNA polymerase II-dependent transcription of enhancers.**

INTRODUCTION

During development, somatic progenitor cells engage into differentiation to form organs. In adult tissues, stem cells, which have self-renewal capacities, differentiate to maintain tissue homeostasis or to repair damage. The balance between self-renewal and differentiation has to be tightly controlled to allow adequate development and prevent aberrant growth of tissues. The switch between self-renewal and differentiation states is associated with profound changes in gene expression and global genomic rearrangements. Activation and repression of enhancer elements embedded in chromatin are instrumental to orchestrate these changes. Extensive studies of the role of chromatin modifications in the regulation of cell stemness and differentiation have demonstrated the importance of histone modifications, and enzymes involved in the control of lysine methylation have particularly emerged as key regulators of cell fate (Agger et al., 2007; Amente et al., 2013; Pereira et al., 2010; Rajasekhar and Begemann, 2007; Zylicz et al., 2015).

Lysine-specific demethylase 1 (LSD1, AOF2, KDM1A) is a monoamine oxidase that can de-methylate mono- and di-methylated lysine 4 and 9 residues of the N terminus of histone H3 (H3K4Me1, H3K4Me2 and H3K9Me1, H3K9Me2), thus promoting either transcriptional repression or activation (Metzger et al., 2005; Mulligan et al., 2011; Shi et al., 2004; Yang et al., 2006). Whole-genome distribution studies have shown that, in stem cells, LSD1 preferentially localizes at enhancers, where it represses the enhancers involved in stemness maintenance at the onset of differentiation (Whyte et al., 2012). Functional approaches using *Lsd1* inactivation in mice have also demonstrated the involvement of LSD1 in the engagement of progenitor cells into differentiation (Wang et al., 2007). The requirement of LSD1 for differentiation of progenitor cells can be explained by the need to decommission stemness enhancers to allow differentiation (Whyte et al., 2012). One of the best-characterized examples of how progenitor cells multiply and differentiate to form functional organs is myogenesis. The complex signaling and transcriptional cascades that control the specific timing of expression of muscle-specific regulatory genes have been extensively studied. Among these factors, MYOD is a key regulator of the engagement into differentiation of muscle progenitor cells (Conerly et al., 2016; Tapscott et al., 1988). Contrary to the abundant knowledge accumulated on how MYOD affects chromatin organization to promote muscle cell differentiation (Bergstrom et al., 2002; Berkes and Tapscott, 2005; de la Serna et al., 2005; Forcales et al., 2012; Sartorelli et al., 1997; Tapscott,

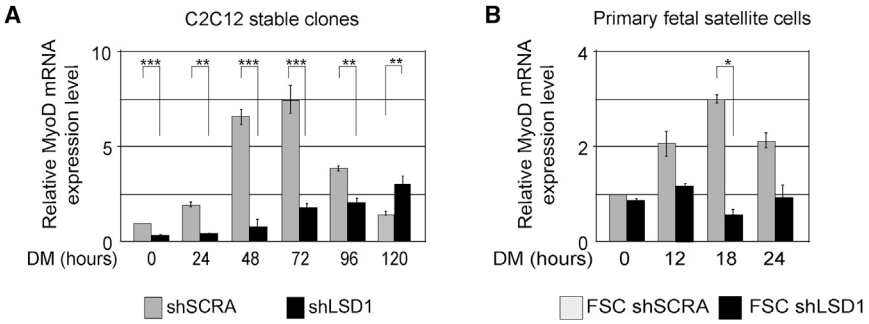

Figure 1. Inhibition of Lsd1 in Cultured Myoblasts Drastically Reduces MyoD Expression

(A and B) *MyoD* mRNA levels in shSCRA and shLSD1 cells (A) and primary fetal satellite cells (B) infected with a scrambled shRNA or an shRNA against LSD1 (FSC shSCRA and FSC shLSD1, respectively) during differentiation. Real-time qPCR values were normalized to the *Ppib* mRNA. mRNA levels are shown as the fold variation compared with shSCRA or FCS shSCRA cells at differentiation medium 0 hours (DM0).

Data are represented as mean ± SEM of at least three experiments. $^{**}p < 0.01$, $^{***}p < 0.001$ (Bonferroni test after one-way ANOVA). See also Figures S1–S3.

2005), the chromatin changes on the *MyoD* promoter that trigger *MyoD* expression still lack in-depth understanding. Among the regulatory regions of *MyoD*, the core enhancer (CE) region, located about 25 kb upstream of the MyoD promoter, has been demonstrated to control the initiation of *MyoD* expression during myoblast commitment (Asakura et al., 1995; Chen and Goldhamer, 2004; Chen et al., 2001; Goldhamer et al., 1995). Recent findings regarding the transcriptional initiation of the *MyoD* gene have shown that many different factors bind the CE (Andrews et al., 2010; L'honoré et al., 2010; Relaix et al., 2013). Moreover, involvement of epigenetic remodeling in the activation of the CE has been demonstrated by in vitro studies that showed the requirement of histone variant H3.3 deposition on the CE for proper expression of *MyoD* in differentiating myoblasts (Yang et al., 2011). Consistent with the association of H3.3 with transcriptionally active regions, it has been discovered that the CE region was transcribed to produce a non-coding RNA enhancer (CEeRNA) playing a key role in *MyoD* expression during early differentiation steps (Mousavi et al., 2013).

On this basis, we decided to investigate the possibility that LSD1 could positively or negatively regulate the core enhancer of MyoD and, therefore, the initiation of *MyoD* expression in muscle precursor cells. LSD1 inhibition in myoblasts drastically decreased *MyoD* upregulation, indicating that LSD1 might be involved in MyoD expression control. Further functional and chromatin immunoprecipitation (ChIP) experiments revealed that, upon induction of differentiation, LSD1 was recruited on the *MyoD* core enhancer, where it promoted the expression of the CEeRNA, which, consequently, controlled the timely transcription of *MyoD*. Finally, the involvement of LSD1 in the regulation of CEeRNA expression during myogenesis was provided by conditional inactivation of *Lsd1* in muscle precursor cells using a Pax3-cre knockin mouse strain (Engleka et al., 2005; Li et al., 2000). LSD1 conditional inactivation in PAX3-positive cells recapitulated the effect of the deletion of the MyoD core enhancer (Chen and Goldhamer, 2004; Chen et al., 2001). The expression of the CEeRNA and *MyoD* in the forelimbs on embryonic day 10.5 (E10.5) was drastically reduced. Altogether, our results indicate that, during muscle cell commitment, LSD1 is necessary for *MyoD* core enhancer expression. LSD1 is required to prevent H3K9 tri-methylation and recruit RNA polymerase II for the transcription of an essential non-coding RNA enhancer.

RESULTS

LSD1 Inhibition in Cultured Myoblasts Prevents Differentiation by Affecting the Timely Increase of *MyoD* Expression

During C2C12 myoblast differentiation, an increase in LSD1 protein level was observed and coincided with that of MYOD protein and mRNA levels (Figure S1). Thus, we asked whether LSD1, by modulating *MyoD* expression, could play a role in the entry of muscle cells into the differentiation process.

To test our hypothesis, LSD1 activity was inhibited in cultured myoblasts with the two LSD1 inhibitors Pargyline and OG-L002 (Figures S2A and S2B; Choi et al., 2010; Liang et al., 2013; Metzger et al., 2005). After 72 hr in differentiation medium (DM), C2C12 myoblasts treated with Pargyline or OG-L002 showed a dose-dependent decrease in *MyoD* expression (Figure S2C), indicating that LSD1 de-methylase activity was required for the increase in *MyoD* expression. To further investigate the mechanism of action of LSD1 in *MyoD* transcription, C2C12 cells were stably transduced with a lentivirus expressing either a short hairpin RNA (shRNA) directed against LSD1 (shLSD1) or a control shRNA (shSCRA) (Figure S3A). Consistent with previous reports (Choi et al., 2010; Munehira et al., 2016), although shSCRA and shLSD1 cells had identical growth rates (Figure S3B) and reached the same density after 72 hr in DM (Figure S3C), shLSD1 cells showed a marked reduction in their ability to fuse and form myotubes (Figure S3D). Only 3% of shLSD1 cells underwent fusion, with the majority of myotubes containing only two to five nuclei, whereas 63% of shSCRA myoblasts formed myotubes, most of them containing more than ten nuclei (Figures S3E and S3F). As reported previously, this lack of differentiation was paralleled by a reduction of both Myogenin protein (Figure S3G) and mRNA levels (Figure S3H; Cheng et al., 2014; Choi et al., 2010). In addition, shLSD1 cells as well as primary fetal satellite cells (FSCs) transiently infected with LSD1 shRNA showed a dramatic decrease in *MyoD* mRNA level (Figures 1A and 1B), strongly suggesting that LSD1 and its catalytic activity are required at early stages of differentiation to upregulate *MyoD* expression.

LSD1 Is Recruited on the *MyoD* Core Enhancer during Differentiation

So far, three regulatory regions have been identified to independently control *MyoD* expression: the proximal promoter, the

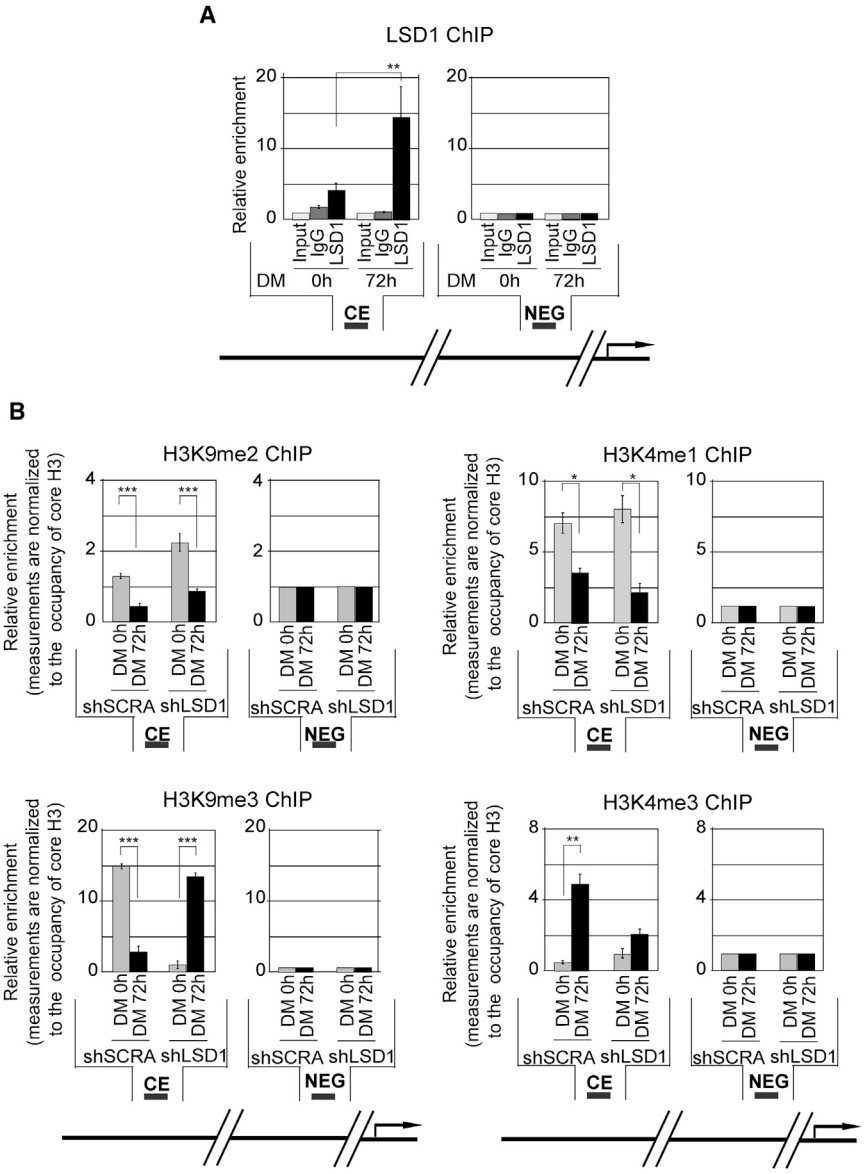

Figure 2. LSD1 Recruitment on the *MyoD* Core Enhancer Region Correlates with Its Activation

(A) Localization of LSD1 at the CE region of the *MyoD* gene locus after 72 hr in DM. ChIP analysis was performed on shSCRA cells with an anti-LSD1 antibody. Enrichment values were normalized to input.

(B) ChIP analysis of the CE region on shSCRA and shLSD1 cells at DM0 and after 72 hr in DM using antibodies against H3K9me2, H3K9me3, H3K4me1, and H3K4me3. Enrichment values were normalized to input and to the occupancy of the core H3. Two sites, CE and NEG, were tested for real-time qPCR amplification.

Data are shown as fold difference relative to the NEG region and represented as mean ± SEM of at least three experiments. $^{**}p < 0.01$, $^{***}p < 0.0005$ (Bonferroni test after one-way ANOVA). See also Figure S4.

distal regulatory region (DRR), and the CE (Asakura et al., 1995; Goldhamer et al., 1995). Although the DRR is required to maintain *MyoD* expression in differentiating muscle cells, the CE region controls the initiation of *MyoD* expression in newly determined myoblasts, (Asakura et al., 1995; Chen et al., 2001; Goldhamer et al., 1995). To further examine the regulatory role of LSD1 on *MyoD* transcription, we performed ChIP experiments on shSCRA myoblasts. In our in vitro model, 72 hr after switching cells to DM, *MyoD* expression reached its maximum, and myoblasts were committed to differentiate, as evidenced by *Myogenin* expression (Figure 1A; Figures S1A, S1B, and S3C). At that time, LSD1 was strongly enriched at the *MyoD* core enhancer (Figure 2A; Figure S4).

Furthermore, the presence of LSD1 on the CE coincided with a reduction in the H3K9me2 and H3K9me3 repressive marks along with a reduction in H3K4me1. Similar ChIP experiments performed on shLSD1 myoblasts placed for 72 hr into DM showed that, contrary to what we observed in shSCRA cells, the H3K9me3 repressive mark did not only fail to decrease but strongly increased in shLSD1 cells (Figure 2B).

Previous ChIP sequencing (ChIP-seq) studies have suggested that transcriptional enhancers are associated with high levels of H3K4me1 (Heintzman et al., 2009). Pekowska et al. (2011) further demonstrated that H3K4me1 is not indicative of enhancer activity but that there is a functional link between enhancer activity and H3K4me3 enrichment. Interestingly, the presence of LSD1 positively correlates with a strong increase in the activation mark H3K4me3 (Figure 2B) in that region after 72 hr in DM. Consistently, by analyzing two published ChIP-seq datasets (Asp et al., 2011; Mousavi et al., 2012), we observed an enrichment of H3K4me3 in the CE region during myoblast differentiation (data not shown). Altogether, these results point to a central role of LSD1 in the activation of the CE region.

LSD1 Participates in the Activation of CEeRNA Transcription

Activation of the CE region was recently shown to trigger the transcription of the CEeRNA that improves the recruitment of RNA polymerase II (RNApolII) on the *MyoD* proximal promoter and, thus, participates to the timely increase of *MyoD* expression and myoblast differentiation (Mousavi et al., 2013). A possible role of LSD1 in the transcription of the CEeRNA was investigated. Seventy-two hours in DM induced a significant increase of the of CEeRNA level in shSCRA cells (Figure 3A), whereas it remained unchanged in shLSD1 cells as well as in myoblasts

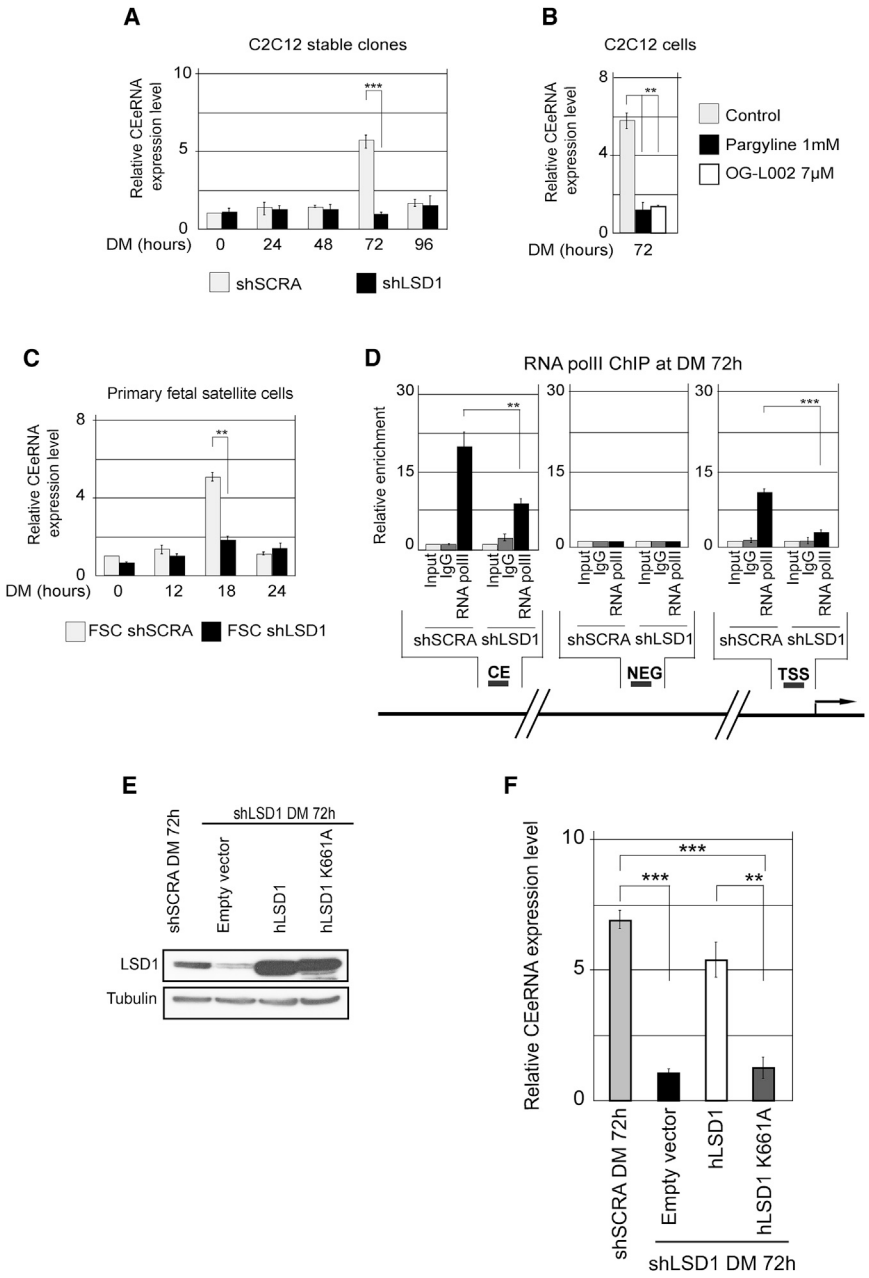

Figure 3. Demethylase Activity of LSD1 Is Required to Promote CEeRNA Transcription

(A–C) CEeRNA expression in shSCRA and shLSD1 cells (A), control C2C12 cells treated with pargyline or OG-L002 (B), and FSC shSCRA and FSC shLSD1 (C). Real-time qPCR values were normalized to the *Ppib* mRNA levels and are shown as the fold difference with DM0.

(D) Localization of RNApolII at the *MyoD* gene locus. ChIP analysis was performed on shSCRA and shLSD1 cells after 72 hr in DM with an anti-RNApolII antibody. Three sites, CE, NEG, and TSS, were tested for real-time qPCR amplification. Enrichment values were normalized to input and are shown as the fold difference relative to the NEG region.

(E) Western blot analysis of LSD1 protein levels after 72 hr in DM in shSCRA, shLSD1, and shLSD1 cells expressing wild-type or hLSD1 K661A hLSD1.

(F) CEeRNA expression after 72 hr in DM in shSCRA, shLSD1, and shLSD1 cells expressing wild-type or hLSD1 K661A hLSD1. Real-time qPCR values were normalized to the *Ppib* mRNA levels and are shown as the fold difference with shSCRA at DM0.

Data are represented as mean ± SEM of at least three experiments. $^{**}p < 0.01$, $^{***}p < 0.0005$ (Bonferroni test after one-way ANOVA).

treated with Pargyline or OG-L002 (Figure 3B). Accordingly, FSCs transduced with LSD1 shRNA (Figure 3C) failed to activate CEeRNA expression during differentiation. Consistently, RNApolII was less enriched on the CE and near the *MyoD* transcription start site (TSS) in shLSD1 cells than in shSCRA myoblasts after 72 hr in DM (Figure 3D).

To ensure that the inhibition of CEeRNA expression was due to the knockdown of LSD1, rescue experiments were performed by expressing either a human wild-type LSD1 (hLSD1) or a catalytically inactive LSD1 mutant (hLSD1 K661A; Lee et al., 2006) that are not targeted by the mouse LSD1 shRNA (Figure 3E). Expression of hLSD1 efficiently restored the expression of the CEeRNA after 72 hr in DM in shLSD1 cells. Conversely, the hLSD1 K661A mutant failed to rescue CEeRNA expression (Figure 3F). These results demonstrate the requirement of LSD1 and of its de-methylase activity for the activation of CEeRNA expression.

To determine whether allowing transcription of the CEeRNA is the main function of LSD1 in the activation of MyoD expression, the CEeRNA was overexpressed in shLSD1 cells, and their ability to differentiate was explored. ShLSD1 myoblasts were transfected with either an empty vector or CEeRNA expression vectors (Figure 4A; Figure S5A). After 72 hr in DM, examination of *MyoD* mRNA levels revealed that neither the empty vector nor the vector containing the CEeRNA cloned in the + orientation rescued *MyoD* expression in shLSD1 cells (Figure 4B). Conversely, in shLSD1 cells transfected with the vector expressing the CEeRNA (– strand), *MyoD* expression was restored to the same level as in shSCRA cells (Figure 4B). Consistently, MYOD protein levels were also restored in these cells (Figure 4C; Figures S5B and S5C). Moreover, expression of the CEeRNA (– strand) in shLSD1 cells allowed a 10-fold improvement of their ability to form myotubes (Figures 5A and 5B). Indeed, 30% of the cells fused to form myotubes with an average of six to ten nuclei per myotube, whereas only 3% of the shLSD1 cells transfected

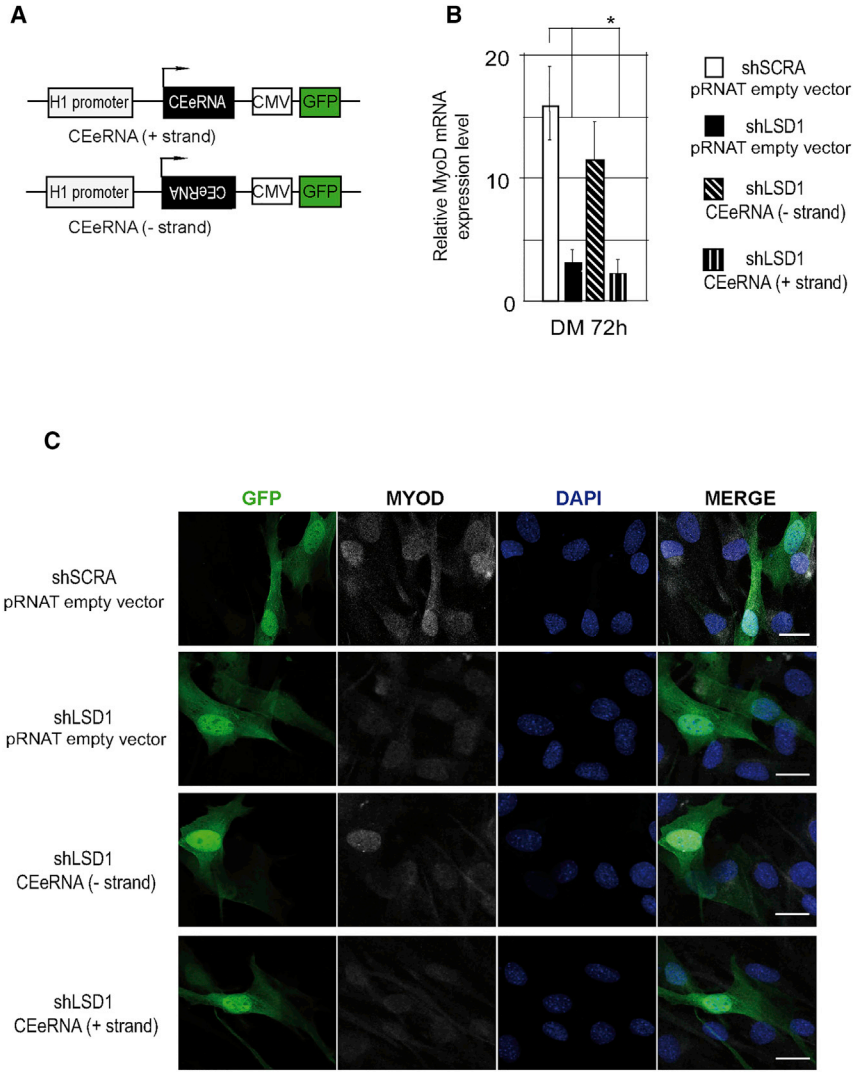

Figure 4. LSD1-Driven CEeRNA Expression Is Required for *MyoD* Expression

(A) Schematic of pRNAT constructs expressing the CEeRNA used in the rescue experiment.

(B) *MyoD* mRNA levels in shSCRA transiently transfected with empty pRNAT vector and in shLSD1 cells transiently transfected with empty pRNAT vector and CEeRNA (– strand) or (+ strand) vectors after 72 hr in DM. Real-time qPCR values were normalized to the *Ppib* mRNA levels and are shown as the fold difference with shSCRA at DM0. Data are represented as mean ± SEM of at least three experiments. *$p < 0.05$ (Bonferroni test after one-way ANOVA).

(C) Confocal pictures showing MYOD immunostaining in shSCRA myoblasts transiently transfected with pRNAT empty vector and in shLSD1 cells transiently transfected with pRNAT empty, CEeRNA (– strand), or CEeRNA (+ strand) vectors after 72 hr in DM. Scale bar, 20 μm. Data are representative of at least three independent experiments.

See also Figure S5.

with the empty or CEeRNA (+ strand) vectors underwent fusion (Figures 5B and 5C). In conclusion, our data demonstrate that LSD1 controls *MyoD* expression during myoblast differentiation via activation of CEeRNA transcription.

Lsd1 Inactivation in Muscle Precursor Cells Prevents the Timely Expression of *MyoD*

The CE region upstream of the *MyoD* locus has long been known to control the spatiotemporal pattern of expression of *MyoD* during embryogenesis (Chen and Goldhamer, 2004; Chen et al., 2001). In vivo, removing the core enhancer from the *MyoD* regulatory regions induces a temporary inhibition of *MyoD* expression. On E11.5, a mild reduction in *MyoD* expression in the somites and a major impairment of *MyoD* expression in the forelimbs can be observed, indicating that, in the forelimb region, *MyoD* expression is core enhancer-dependent (Chen and Goldhamer, 2004). One day later, *MyoD* expression is back to normal (Chen and Goldhamer, 2004; Chen et al., 2001). LSD1 immunofluorescence on E11.5 control embryo transverse sections showed that LSD1 was more expressed in muscle progenitors (PAX3-positive cells) in the forelimb than in the somite region (Figure 6A). To evaluate the requirement of LSD1 for CE dependent-*MyoD* expression in vivo, we conditionally ablated *Lsd1* in muscle progenitors (*LSD1 cKO*; Figure S6A) by crossing Lsd1^{tm1Schüle} mice carrying a new conditional allele for *Lsd1* deletion engineered by the Schüle group (Zhu et al., 2014) and *Pax3*$^{Cre/+}$ mice (Engleka et al., 2005; Li et al., 2000). In situ hybridization on E11.5 *LSD1 cKO* embryos showed that LSD1 inactivation in muscle progenitor cells resulted in a mild and strong temporary impairment of *MyoD* expression in the somites and in the forelimbs, respectively (Figure 6B). Indeed, on E12.5, *MyoD* expression was restored to the same levels as observed in control embryos (Figure 6B). In vivo ablation of LSD1 fully mimics that of the core enhancer. Of note, other PAX3-expressing cells, such as the neural crest-derived lineage, were not affected, as seen with *Sox10* expression (Figure S6B). To confirm *MyoD* downregulation, western blot experiments were performed on E11.5 *LSD1 cKO* and control embryo total protein extracts. The MYOD protein level was reduced in the absence of LSD1 (Figure S6C). No alterations of PAX7 and MYF5 protein levels were observed (Figure S6C), supporting the idea that, at early stages of muscle progenitor differentiation, LSD1 specifically controls *MyoD* expression but does not affect the expression of other early myogenic determination factors. This would explain why, in the absence of MYOD (Conerly et al., 2016; Rawls et al., 1998) and LSD1, myogenesis is delayed but ultimately proceeds. To evaluate the effect of LSD1 inactivation on the proportion of progenitors that turned on *MyoD* expression, MYOD- and PAX3-positive cells in the

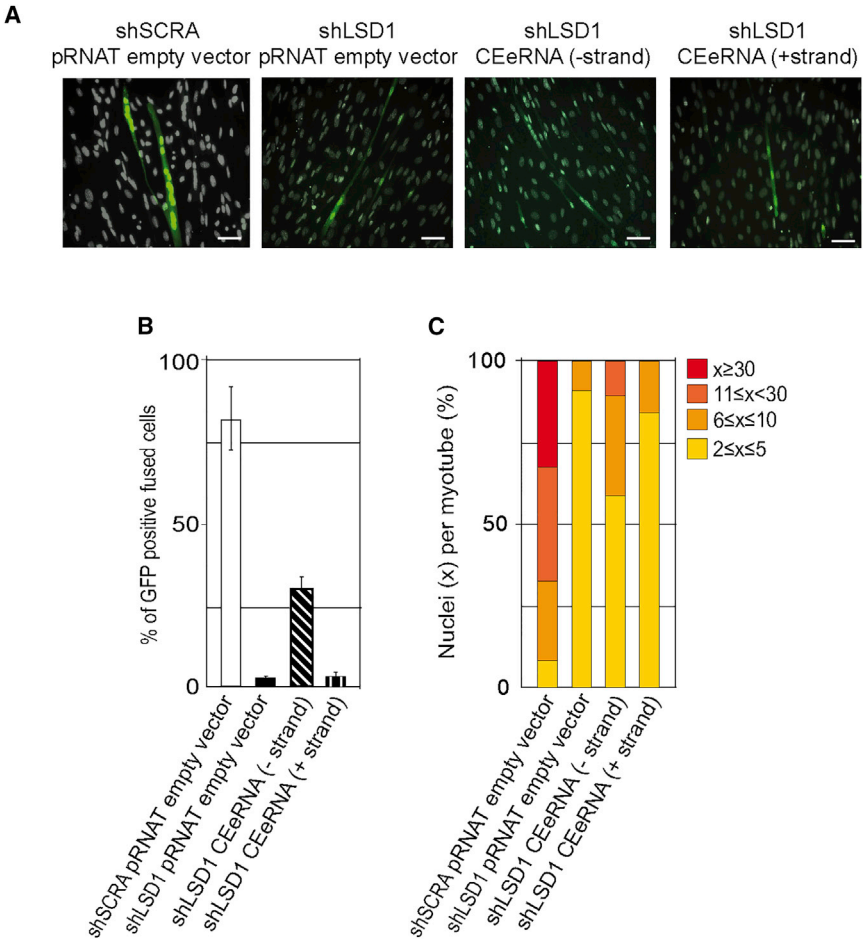

Figure 5. CEeRNA Minus Strand Overexpression Rescues Myotube Formation in the Absence of LSD1

(A) Representative images of shSCRA transiently transfected with empty pRNAT vector, shLSD1 transiently transfected with empty pRNAT vector, and CEeRNA (+ strand) or CEeRNA (– strand) cells after 120 hr in DM. Scale bars, 50 μm.

(B) The percentage of fused cells was calculated as the proportion of GFP-positive cells containing two or more nuclei.

(C) Nuclei were counted in shLSD1 cells transfected with pRNAT empty, CEeRNA (– strand), or CEeRNA (+ strand) (180, 132, and 102 cells, respectively) vectors and in 110 shSCRA cells transfected with pRNAT empty vector. The graphs represent three different experiments.

forelimb of E11.5 embryos were visualized by immunofluorescence. Counting PAX3- and MYOD-positive cells revealed that the percentage of MYOD-positive cells in the forelimb on E11.5 was significantly lower in *LSD1 cKO* compared with the control (Figure 6C). Consistent with the delay in *MyoD* expression and with the previously reported role of LSD1 on *Myogenin* activation (Cheng et al., 2014; Choi et al., 2010), a strong reduction in *Myogenin* expression was observed in LSD1 cKO forelimbs on E11.5 (Figures S6C and S6D).

Lsd1 Inactivation in Muscle Precursor Cells Prevents CEeRNA Expression

In vitro results indicated that the control of MyoD expression by LSD1 was mediated by expression of the CEeRNA. CEeRNA expression was therefore evaluated in E10.5 control and LSD1 cKO embryos, both by in situ hybridization and by real-time qPCR on dissected forelimbs. Both approaches showed that, in LSD1 cKO embryo forelimbs, CEeRNA and *MyoD* mRNA levels were dramatically reduced (Figures 7A and 7B; Figure S7B). Consistent with our in vitro results, only the CEeRNA (– strand) was significantly expressed in the forelimb region (Figure S7A). These results demonstrate that, in vivo, LSD1 is essential for MyoD core enhancer transcription in muscle cell commitment.

DISCUSSION

Although the action of MYOD on chromatin remodeling during muscle differentiation has been extensively studied, still little is known about the chromatin remodeling events associated with the increase in *MyoD* expression. The core enhancer of *MyoD* is required for the initiation of *MyoD* expression in newly determined myoblasts (Asakura et al., 1995; Chen and Goldhamer, 2004; Chen et al., 2001; Goldhamer et al., 1995). In this work, we have demonstrated that LSD1 is required for the transcription of the CEeRNA from the core enhancer region. So far, LSD1 is the first chromatin-modifying enzyme identified to regulate the activity of the core enhancer of MyoD.

The inhibition of myoblast differentiation and of CEeRNA expression by two different LSD1 pharmacological inhibitors (Pargyline and OG-L002) or a catalytically inactive LSD1 mutant shows that LSD1 enzymatic activity is required to increase *MyoD* expression. However, the loss of H3K9 tri-methylation cannot be directly attributed to LSD1 enzymatic activity, suggesting that LSD1 might work together with other histone de-methylases to prevent H3K9 tri-methylation upon differentiation. Consistently, the absence of LSD1 in differentiating myoblasts induced a strong increase in H3K9 tri-methylation (Figure 2B). Increased H3K9me3 in the absence of LSD1 could be due to the fact that LSD1 prevents H3K9 tri-methylation by removing mono- and di-methylation and/or that LSD1 prevents the recruitment/activity of a methyl transferase. This possibility would fit with the idea that LSD1 belongs to large multiprotein complexes and could affect the composition of the complexes recruited on the core enhancer.

Indeed, the function of histone de-methylases is not only defined by their active site. Both interactions with the histone substrates and with protein partners can profoundly affect substrate specificity and activity (Cai et al., 2014; Metzger et al., 2005, 2010; Shi et al., 2005). In addition, LSD1 could

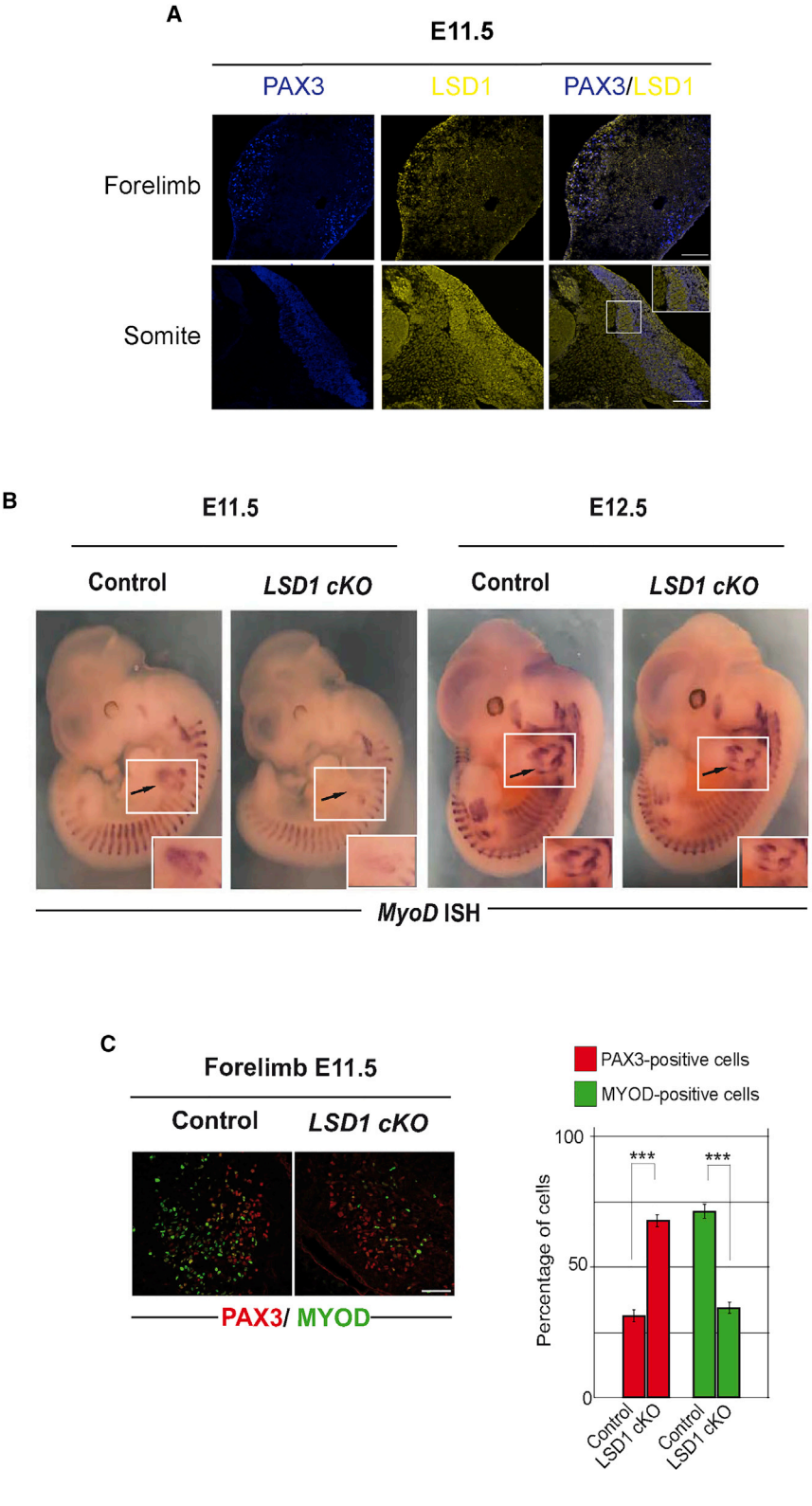

Figure 6. LSD1 Depletion Spatio-temporally Impairs *MyoD* Expression during Embryogenesis

(A) LSD1 and PAX3 immunostaining of transverse sections of E11.5 control embryos in the forelimb and somite regions. Scale bars, 100 μm.

(B) Whole-mount in situ hybridization for *MyoD* mRNA in control and *LSD1 cKO* embryos on E11.5 and E12.5. The insets show a higher magnification of the forelimb.

(C) PAX3 and MYOD immunostaining in the forelimbs of E11.5 control and LSD1 cKO embryos. Scale bar, 50 μm. Right: quantification of the relative proportion of PAX3- and MYOD-positive cells in control and *LSD1 cKO* forelimb (left) and data are expressed as percentage over the total immunostained cell population.

Histogram data are mean ± SEM. ***$p < 0.01$ ($n = 3$ embryos for each condition) (Bonferroni test after one-way ANOVA). See also Figure S6.

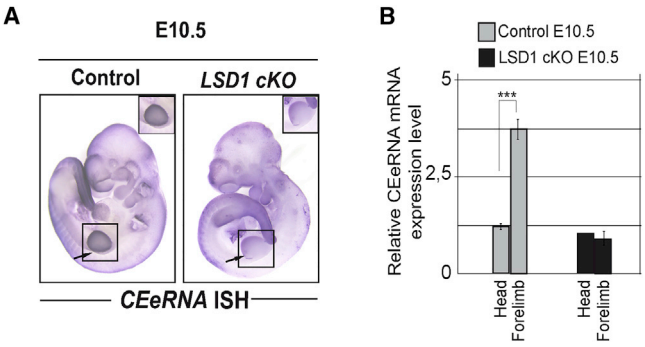

Figure 7. LSD1 Depletion Impairs CEeRNA Expression In Vivo on E10.5

(A) Whole-mount in situ hybridization for CEeRNA using a sense probe in control and *LSD1 cKO* embryos on E10.5. The insets show a higher magnification of the forelimb region.

(B) CEeRNA level in dissected forelimbs and heads from control and LSD1 cKO embryos on E10.5. Real-time qPCR values were normalized to the *Ppib* mRNA levels and are shown as the fold difference with control head. ***$p < 0.0001$ (six control and four LSD1 cKO embryos) (Bonferroni test after one-way ANOVA).

See also Figure S7.

also de-methylate non-histone substrates, such as components of co-activator complexes. Regarding H3K4 methylation, as part of co-activator complexes LSD1 could favor RNA polymerase II recruitment, which comes along with the complex proteins associated with Set1 (COMPASS) complex that catalyzes H3K4 tri-methylation (Dehé and Géli, 2006; Terzi et al., 2011). In the absence of LSD1, RNA polymerase II recruitment on the *MyoD* core enhancer is reduced, and the level of H3K4 tri-methylation is strongly impaired, indicating that LSD1 could be required for RNA polymerase II recruitment on the core enhancer of *MyoD*.

Mousavi et al. (2013) have shown that transcription of the core enhancer by RNA polymerase II generated a non-coding enhancer RNA that promoted the recruitment of RNA polymerase II on the proximal promoter of MyoD. However, which strand of the CEeRNA had to be transcribed to regulate *MyoD* transcription remained unknown. Our results show that only the transcription of the minus strand of the CEeRNA promotes *MyoD* transcription and that, in forelimbs, only this strand is expressed. Whether this is due to unidirectional transcription of the core enhancer or different stabilities of the RNA transcribed from the plus and minus strands remains an open question.

Recently, LSD1 was shown to bind and activate enhancers stimulated by androgen receptors (AR-stimulated enhancer) (Cai et al., 2014). However, the mechanism described in that case was different from the one we report here. While activating the transcription of AR-dependent genes, LSD1 still catalyzed H3K4 de-methylation on AR-stimulated enhancers. Our study shows that LSD1 can have a different enhancer-activating activity that involves H3K4 methylation via RNA polymerase II recruitment on the transcribed enhancer.

Several observations argue in favor of the idea that the main function of LSD1 during muscle cell engagement is the timely control of *MyoD* expression via activation of the CEeRNA: the LSD1 inactivation effect can be efficiently rescued by the expression of the CEeRNA (− strand), LSD1 inactivation in mouse muscle progenitors inhibits the expression of the CEeRNA and mimics the *MyoD* core enhancer deletion phenotype, and LSD1 inactivation does not interfere with the alternative mechanisms that allow delayed muscle differentiation in the absence of *MyoD*. Indeed, the expression of other muscle determination factors such as PAX7 and MYF5 is not affected by the inactivation of LSD1.

The specific action of LSD1 in the early steps of differentiation does not exclude the possibility that LSD1 may also be involved in later stages of muscle differentiation. Indeed, LSD1 has been shown to directly regulate *Myogenin* expression in cultured myoblasts (Cheng et al., 2014; Choi et al., 2010). This could explain why, in rescue experiments with the CEeRNA, *Myogenin* expression is only partially rescued (Figure S5B). This would also explain why, although expression of the CEeRNA efficiently restored myoblast fusion in the absence of LSD1, myotubes remained thinner and incorporated fewer nuclei than control cells (Figure 5).

In conclusion, our data show that LSD1 is required for the timely expression of *MyoD* via activation of the *MyoD* core enhancer. More generally, our results indicate that, in addition to repress stemness enhancers, LSD1 can participate in cell engagement into differentiation by activating pro-differentiation enhancers. This raises the question of the mechanisms that drive LSD1 to selectively silence stemness enhancers and/or activate pro-differentiation enhancers upon progenitor cell commitment.

EXPERIMENTAL PROCEDURES

Cell Lines, Culture Conditions, Infection, and Transfection

C2C12 mouse myoblasts were maintained as myoblasts in growth medium (GM): Dulbecco's modified Eagle's medium supplemented with 15% fetal calf serum and antibiotics. Primary FSCs were maintained on Matrigel-coated dishes in GM: Dulbecco's modified Eagle's medium F12 supplemented with 20% fetal calf serum, 5 ng/mL fibroblast growth factor (FGF), and antibiotics. C2C12 cells and FSC cells were differentiated into myotubes by replacing GM with medium containing 2% horse serum with antibiotics (DM). For stable knockdown of *Lsd1* in C2C12 cells, a lentiviral vector containing the mouse Lsd1-targeting sequence pLKO.1-sh-LSD1 (TRCN0000071377, ShLSD1), purchased from Open Biosystem, was used. As an shSCRA, the pLKO.1 vector SHC016V, purchased from Sigma-Aldrich, was used. Twenty-four hours after lentiviral infection, C2C12 were selected with puromycin (1 μg/mL) for 14 days. To avoid problems with clonal variation, all clones (50–100/transfection) were pooled and then used for experiments.

Primary fetal satellite cells were infected with the pLKO.1-sh-LSD1 (FSC shLSD1) and the pLKO.1 vector SHC016V (FSC shSCRA). Twenty-four hours after lentiviral infection, FSCs were induced to differentiate.

Pargyline (1 mM) and OG-L002 (5 μM, 7 μM, or 10 μM) were added to C2C12 cells concomitant with DM and again 48 hr thereafter.

Cell transfections with the pRNAT vector (pRNAT-CMV3.1/Neo by GenScript), CEeRNA vectors were performed as follows: 300,000 shSCRA and shLSD1 cells were seeded in 35-mm petri dishes. Three hours later, shSCRA cells were transfected with pRNAT empty vector, and shLSD1 cells were transfected with pRNAT empty vector or CEeRNA (+ strand) or CEeRNA (− strand) with jetPRIME (polyplus transfection) according to the manufacturer's instructions. Twenty-four hours after transfection, cells were seeded (150,000 cells/35-mm petri dishes) in DM for 72 hr for RNA or protein analysis and 120 hr for nucleus counting. Cell transfections with hLSD1 and hLSD1 K661A plasmids were performed as described previously. Twenty-four hours after transfection, cells were seeded (150,000 cells/35-mm petri dishes) in DM for 72 hr for RNA or protein analysis.

Cloning

CEeRNA constructs were generated with Phusion Green High-Fidelity DNA Polymerase (Thermo Scientific) and confirmed by DNA sequencing. The full-length CEeRNA was cloned in the pRNAT vector (pRNAT-CMV3.1/Neo by GenScript) in the sense (CEeRNA [+ strand]) and antisense (CEeRNA (− strand]) orientations under the control of the strong H1 promoter using the BAMHI site. For oligonucleotides details, see the Supplemental Experimental Procedures.

Real-Time qPCR

Total RNA was isolated from cultured cells grown in 100-mm dishes using Trireagent (Sigma). RNA was analyzed by real-time PCR using the QuantiFast SYBR Green PCR Kit (QIAGEN). Relative gene expression was determined using the ΔCt method. Total RNA from dissected forelimbs and heads of control and LSD1cKO embryos on E10.5 was isolated using the RNeasy Micro Kit (QIAGEN) according to the manufacturer's instructions. For oligonucleotide details, see the Supplemental Experimental Procedures.

Immunoblotting

Proteins were extracted from total embryos and cells and quantified using the DC protein assay (Bio-Rad). Total proteins were separated by 10% SDS-PAGE electrophoresis and transferred onto polyvinylidene fluoride (PVDF) Immobilon-P membranes (Millipore). Immunoblots were performed with enhanced chemiluminescence (ECL) PLUS reagent (Amersham or GE Healthcare) according to the manufacturer's instructions. For antibodies details, see the Supplemental Experimental Procedures.

ChIP

1×10^7 C2C12 cells were incubated in 1% formaldehyde on a rotating wheel for 10 min at room temperature. Reactions were stopped by adding glycine at a final concentration of 0.125 M and incubated on a rotating wheel for 10 min at room temperature. After a PBS wash, the pellet was dissolved in ice-cold cell lysis buffer (5 mM PIPES, 85 mM KCl, and 0.5% NP40) and incubated on ice for 10–20 min. Nuclei were centrifuged at 3,000 rpm for 5 min at 4°C, dissolved in ice-cold radio immunoprecipitation assay (RIPA) (150 mM NaCl, 0.5% NaDoc, 1% NP40, 0.1% SDS, and 50 mM TrisHCl) buffer and incubated on ice for 10–20 min. Nuclei were sonicated with a Bioruptor PLUS combined with the Bioruptor water cooler (Diagenode). The size of chromatin fragments was checked. Chromatin was then pre-cleared by incubation with protein A-Sepharose 4B fast flow (Sigma) for 15 min at 4°C with constant rotation. After centrifugation, specific antibodies were added and rotated overnight at 4°C. Protein A-Sepharose 4B fast flow (Sigma) was added and incubated with constant rotation for 30 min at room temperature. Beads were then washed, and chromatin IP was de-cross-linked with Proteinase K at 65°C for 6 hr. Chromatin IP and INPUT were extracted and dissolved in 10 mM TrisHCl (pH 8). Three sites, CE, negative [NEG], and TSS, were tested for real-time qPCR amplification. Real-time qPCR data analysis for LSD1 and RNApolII IPs has been performed by calculating the percentage of input for each genomic region; data are shown as the relative enrichment to the control genomic region (NEG region) that does not interact with the protein of interest. Real-time qPCR data analysis for H3, H3K9me2, H3K9me3, H3K4me1, and H3K4me3 IPs has been performed as described previously. Data were also normalized to the occupancy of H3 in each genomic region and shown as the relative enrichment to the control genomic region (NEG region). For oligonucleotides details, see the Supplemental Experimental Procedures.

Nucleus Counting and Percentage of Fusion

The nucleus counting of myotubes was performed as follows. 300,000 shSCRA and shLSD1 cells were seeded in 35-mm petri dishes. Three hours later, shSCRA cells were transfected with pRNAt empty vector, and shLSD1 cells were transfected with pRNAt empty vector or CEeRNA (+ strand) or CEeRNA (− strand). 24 hr after transfection, cells were seeded (150,000 cells/35-mm petri dishes) in DM for 120 hr. Cells were then fixed for 20 min in 4% paraformaldehyde (PFA) in PBS and washed three times in PBS-0.1% Triton X-100 to permeabilize membranes. Cells were then incubated for 20 min with DAPI to stain nuclei and washed three times in PBS. Cells were mounted with Vectashield and observed with a fluorescence microscope (AxioImager).

Mouse Breeding and Embryo Harvesting

Lsd1^{tm1Schüle} and *Pax3*$^{Cre/+}$ mice were described previously (Engleka et al., 2005; Li et al., 2000; Zhu et al., 2014). All mouse handling, breeding, and sacrificing were done in accordance with European legislations on animal experimentation. Experimental mice (*LSD1 cKO*) were generated by crossing *Pax3*$^{Cre/+}$:Lsd1$^{tm1Schüle\ /+}$ males with Lsd1^{tm1Schüle} females. The uterus was removed and placed into dishes filled with PBS. Individual embryos were collected and placed into 4% PFA in PBS overnight at 4°C on a shaker for whole-mount in situ hybridization and immunofluorescence or frozen in liquid nitrogen for protein extraction.

Whole-Mount In Situ Hybridization

Gentle rocking of embryos occurred during the following incubations. Embryos were fixed in 4% PFA in PBS at 4°C overnight. Embryos were rinsed and dehydrated in a gradient of methanol mixed with PBS-T (PBS with 0.1% Tween 20) (25%, 50%, 75%, and 100% methanol) for 10 min each. Embryos were stored at −20°C in 100% methanol until needed. Embryos were returned to room temperature and rehydrated in a reverse gradient in methanol and PBS-T. Embryos were digested with Proteinase K/PBS-T and then fixed in 0.1% glutaraldehyde/4% PFA/PBS-T for 20 min. Following rinses in PBS-T, embryos were incubated in a 1:1 mix of PBS-T and hybridization buffer, followed by 100% hybridization buffer. A digoxigenin-labeled RNA probe (Sassoon et al., 1989) was then added and incubated at 68°C overnight. Embryos were washed in pre-warmed hybridization mix at 68°C. Embryos were then incubated for 10 min at 68°C in a 1:1 mix of hybridization mix and maleic acid buffer with tween 20 (MAB-T) buffer. Embryos were then washed in MAB-T at room temperature and incubated in 2% Boehringer blocking reagent (bbr) in MAB-T for 1 hr at room temperature. Anti-digoxigenin-ap fab fragment (Roche #11093274910) antibody was then added to a 1:2000 dilution and incubated overnight at 4°C. Following incubation with the anti-digoxigenin (DIG) antibody, embryos were washed three times in MAB-T, followed by 3 days of washing in MAB-T, all at room temperature. After replacing NaCl, Tris-cl, MgCl2, Tween-20 (NTMT) with Boehringer Mannheim (BM) purple AP substrate (Sigma-Aldrich, catalog no. 11442074001), color was developed to the appropriate level, usually 6–8 hr. After the color development level was reached, embryos were re-fixed in 4% PFA and stored at 4°C. The *MyoD*, *Myogenin*, and *Sox10* riboprobes were synthesized as described previously (Hayashi et al., 2011; Sassoon et al., 1989). CEeRNA probes were generated by PCR amplification from genomic DNA using the following primers: forward, 5′-GGAGCACCCCACAACATGAGC-3′; reverse, 5′-AGTCTGTGCGGGTGA GGCAG-3′. The resulting 516-bp fragment was subcloned in pGEMT-easy (Promega). Antisense and sense riboprobes were synthesized using the DIG RNA labeling kit (SP6/T7, Sigma).

Immunofluorescence

Embryos and cells were fixed with 4% PFA at 4°C for 2 hr with rotation and at room temperature for 20 min, respectively. The embryos and cells were washed with cold PBS. The fixed embryos were processed through a sucrose gradient of 15% sucrose in PBS overnight, followed by 30% sucrose in PBS overnight. The processed tissue was placed into optimum cutting temperature (OCT) compound and quickly frozen in dry ice-cooled isopentane. The frozen tissues were cryosectioned at 12 μm, washed, and then permeabilized with 100% methanol for 6 min at −20°C. Slides and cells were saturated in PBS, 0.5% Triton X-100, and 5% BSA (PBS-B-T) for 1 hr at room temperature before being stained at 4°C overnight with primary antibodies diluted in PBS-B-T. After three 10-min washes in PBS and 0.1% Triton X-100, slides were incubated for 1 hr at room temperature with secondary antibody diluted in PBS-B-T. After three washes, slides and cells were counterstained with DAPI and mounted. Fluorescent images were acquired on a confocal microscope (Leica TCS SP5) and processed with Photoshop CS4 (Adobe system). For antibodies details, see the Supplemental Experimental Procedures.

Statistical Analysis

Statistical significance was determined by Bonferroni test after one-way ANOVA using GraphPad Prism version 5.00 for Windows (Graph-Pad, http://www.graphpad.com). $p < 0.05$ was considered significant.

SUPPLEMENTAL INFORMATION

Supplemental Information includes Supplemental Experimental Procedures and seven figures and can be found with this article online at http://dx.doi.org/10.1016/j.celrep.2017.01.078.

AUTHOR CONTRIBUTIONS

L.S., F.R., I.S., and E.G. conceived the research. I.S. performed all cell biology, molecular cloning, ChIP, and real-time qPCR experiments and analyses. S.H. carried out the immunofluorescence and in situ hybridization on E11.5 and E12.5 embryos. S.M. performed mouse breeding and embryo harvesting and western blotting on mouse embryos. S.M. and K.A. performed C2C12 myoblast differentiation experiments with LSD1 inhibitors. E.G. performed immunofluorescence on C2C12 cells. J.E.L. performed the in situ hybridization of CEeRNA on E10.5 embryos. V.M. dissected forelimbs and heads from E10.5 embryos. T.S. analyzed the GSE25308 and GSE25549 ChIP-seq data. P.M. and M.W. isolated fetal satellite cells from E18.5 wild-type embryos. E.M. and R.S. generated Lsd1^{tm1Schüle} mice and hLSD1 and hLSD1 K661A constructs. L.S. I.S., and E.G. wrote the manuscript.

ACKNOWLEDGMENTS

Animal breeding and *Lsd1* muscle-specific inactivation were performed at the animal facility (PBES) of the research federation SFR Biosciences (UMS3444). This study was funded by grant Agence Nationale de la Recherche (ANR-11-BSV2-017-01 to L.S. and F.R.) by grants from the European Research Council (ERC AdGrant 322844) and the Deutsche Forschungsgemeinschaft (SFB 992, 850, 746, and Schu688/12-1 to R.S.). I.S. was funded by AFM.

Received: August 14, 2016
Revised: December 21, 2016
Accepted: January 29, 2017
Published: February 21, 2017

REFERENCES

Agger, K., Cloos, P.A., Christensen, J., Pasini, D., Rose, S., Rappsilber, J., Issaeva, I., Canaani, E., Salcini, A.E., and Helin, K. (2007). UTX and JMJD3 are histone H3K27 demethylases involved in HOX gene regulation and development. Nature *449*, 731–734.

Amente, S., Lania, L., and Majello, B. (2013). The histone LSD1 demethylase in stemness and cancer transcription programs. Biochim. Biophys. Acta *1829*, 981–986.

Andrews, J.L., Zhang, X., McCarthy, J.J., McDearmon, E.L., Hornberger, T.A., Russell, B., Campbell, K.S., Arbogast, S., Reid, M.B., Walker, J.R., et al. (2010). CLOCK and BMAL1 regulate MyoD and are necessary for maintenance of skeletal muscle phenotype and function. Proc. Natl. Acad. Sci. USA *107*, 19090–19095.

Asakura, A., Lyons, G.E., and Tapscott, S.J. (1995). The regulation of MyoD gene expression: conserved elements mediate expression in embryonic axial muscle. Dev. Biol. *171*, 386–398.

Asp, P., Blum, R., Vethantham, V., Parisi, F., Micsinai, M., Cheng, J., Bowman, C., Kluger, Y., and Dynlacht, B.D. (2011). Genome-wide remodeling of the epigenetic landscape during myogenic differentiation. Proc. Natl. Acad. Sci. USA *108*, E149–E158.

Bergstrom, D.A., Penn, B.H., Strand, A., Perry, R.L., Rudnicki, M.A., and Tapscott, S.J. (2002). Promoter-specific regulation of MyoD binding and signal transduction cooperate to pattern gene expression. Mol. Cell *9*, 587–600.

Berkes, C.A., and Tapscott, S.J. (2005). MyoD and the transcriptional control of myogenesis. Semin. Cell Dev. Biol. *16*, 585–595.

Cai, C., He, H.H., Gao, S., Chen, S., Yu, Z., Gao, Y., Chen, S., Chen, M.W., Zhang, J., Ahmed, M., et al. (2014). Lysine-specific demethylase 1 has dual functions as a major regulator of androgen receptor transcriptional activity. Cell Rep. *9*, 1618–1627.

Chen, J.C., and Goldhamer, D.J. (2004). The core enhancer is essential for proper timing of MyoD activation in limb buds and branchial arches. Dev. Biol. *265*, 502–512.

Chen, J.C., Love, C.M., and Goldhamer, D.J. (2001). Two upstream enhancers collaborate to regulate the spatial patterning and timing of MyoD transcription during mouse development. Dev. Dyn. *221*, 274–288.

Cheng, J., Blum, R., Bowman, C., Hu, D., Shilatifard, A., Shen, S., and Dynlacht, B.D. (2014). A role for H3K4 monomethylation in gene repression and partitioning of chromatin readers. Mol. Cell *53*, 979–992.

Choi, J., Jang, H., Kim, H., Kim, S.T., Cho, E.J., and Youn, H.D. (2010). Histone demethylase LSD1 is required to induce skeletal muscle differentiation by regulating myogenic factors. Biochem. Biophys. Res. Commun. *401*, 327–332.

Conerly, M.L., Yao, Z., Zhong, J.W., Groudine, M., and Tapscott, S.J. (2016). Distinct Activities of Myf5 and MyoD Indicate Separate Roles in Skeletal Muscle Lineage Specification and Differentiation. Dev. Cell *36*, 375–385.

de la Serna, I.L., Ohkawa, Y., Berkes, C.A., Bergstrom, D.A., Dacwag, C.S., Tapscott, S.J., and Imbalzano, A.N. (2005). MyoD targets chromatin remodeling complexes to the myogenin locus prior to forming a stable DNA-bound complex. Mol. Cell. Biol. *25*, 3997–4009.

Dehé, P.M., and Géli, V. (2006). The multiple faces of Set1. Biochem. Cell Biol. *84*, 536–548.

Engleka, K.A., Gitler, A.D., Zhang, M., Zhou, D.D., High, F.A., and Epstein, J.A. (2005). Insertion of Cre into the Pax3 locus creates a new allele of Splotch and identifies unexpected Pax3 derivatives. Dev. Biol. *280*, 396–406.

Forcales, S.V., Albini, S., Giordani, L., Malecova, B., Cignolo, L., Chernov, A., Coutinho, P., Saccone, V., Consalvi, S., Williams, R., et al. (2012). Signal-dependent incorporation of MyoD-BAF60c into Brg1-based SWI/SNF chromatin-remodelling complex. EMBO J. *31*, 301–316.

Goldhamer, D.J., Brunk, B.P., Faerman, A., King, A., Shani, M., and Emerson, C.P., Jr. (1995). Embryonic activation of the myoD gene is regulated by a highly conserved distal control element. Development *121*, 637–649.

Hayashi, S., Rocancourt, D., Buckingham, M., and Relaix, F. (2011). Lack of in vivo functional compensation between Pax family groups II and III in rodents. Mol. Biol. Evol. *28*, 2787–2798.

Heintzman, N.D., Hon, G.C., Hawkins, R.D., Kheradpour, P., Stark, A., Harp, L.F., Ye, Z., Lee, L.K., Stuart, R.K., Ching, C.W., et al. (2009). Histone modifications at human enhancers reflect global cell-type-specific gene expression. Nature *459*, 108–112.

L'honoré, A., Ouimette, J.F., Lavertu-Jolin, M., and Drouin, J. (2010). Pitx2 defines alternate pathways acting through MyoD during limb and somitic myogenesis. Development *137*, 3847–3856.

Lee, M.G., Wynder, C., Bochar, D.A., Hakimi, M.A., Cooch, N., and Shiekhattar, R. (2006). Functional interplay between histone demethylase and deacetylase enzymes. Mol. Cell. Biol. *26*, 6395–6402.

Li, J., Chen, F., and Epstein, J.A. (2000). Neural crest expression of Cre recombinase directed by the proximal Pax3 promoter in transgenic mice. Genesis *26*, 162–164.

Liang, Y., Quenelle, D., Vogel, J.L., Mascaro, C., Ortega, A., and Kristie, T.M. (2013). A novel selective LSD1/KDM1A inhibitor epigenetically blocks herpes simplex virus lytic replication and reactivation from latency. MBio *4*, e00558–e12.

Metzger, E., Wissmann, M., Yin, N., Müller, J.M., Schneider, R., Peters, A.H., Günther, T., Buettner, R., and Schüle, R. (2005). LSD1 demethylates repressive histone marks to promote androgen-receptor-dependent transcription. Nature *437*, 436–439.

Metzger, E., Imhof, A., Patel, D., Kahl, P., Hoffmeyer, K., Friedrichs, N., Müller, J.M., Greschik, H., Kirfel, J., Ji, S., et al. (2010). Phosphorylation of histone H3T6 by PKCbeta(I) controls demethylation at histone H3K4. Nature *464*, 792–796.

Mousavi, K., Zare, H., Wang, A.H., and Sartorelli, V. (2012). Polycomb protein Ezh1 promotes RNA polymerase II elongation. Mol. Cell *45*, 255–262.

Mousavi, K., Zare, H., Dell'orso, S., Grontved, L., Gutierrez-Cruz, G., Derfoul, A., Hager, G.L., and Sartorelli, V. (2013). eRNAs promote transcription by

establishing chromatin accessibility at defined genomic loci. Mol. Cell *51*, 606–617.

Mulligan, P., Yang, F., Di Stefano, L., Ji, J.Y., Ouyang, J., Nishikawa, J.L., Toiber, D., Kulkarni, M., Wang, Q., Najafi-Shoushtari, S.H., et al. (2011). A SIRT1-LSD1 corepressor complex regulates Notch target gene expression and development. Mol. Cell *42*, 689–699.

Munehira, Y., Yang, Z., and Gozani, O. (2016). Systematic Analysis of Known and Candidate Lysine Demethylases in the Regulation of Myoblast Differentiation. J. Mol. Biol., S0022-2836(16)30419-3.

Pekowska, A., Benoukraf, T., Zacarias-Cabeza, J., Belhocine, M., Koch, F., Holota, H., Imbert, J., Andrau, J.C., Ferrier, P., and Spicuglia, S. (2011). H3K4 tri-methylation provides an epigenetic signature of active enhancers. EMBO J. *30*, 4198–4210.

Pereira, J.D., Sansom, S.N., Smith, J., Dobenecker, M.W., Tarakhovsky, A., and Livesey, F.J. (2010). Ezh2, the histone methyltransferase of PRC2, regulates the balance between self-renewal and differentiation in the cerebral cortex. Proc. Natl. Acad. Sci. USA *107*, 15957–15962.

Rajasekhar, V.K., and Begemann, M. (2007). Concise review: roles of polycomb group proteins in development and disease: a stem cell perspective. Stem Cells *25*, 2498–2510.

Rawls, A., Valdez, M.R., Zhang, W., Richardson, J., Klein, W.H., and Olson, E.N. (1998). Overlapping functions of the myogenic bHLH genes MRF4 and MyoD revealed in double mutant mice. Development *125*, 2349–2358.

Relaix, F., Demignon, J., Laclef, C., Pujol, J., Santolini, M., Niro, C., Lagha, M., Rocancourt, D., Buckingham, M., and Maire, P. (2013). Six homeoproteins directly activate Myod expression in the gene regulatory networks that control early myogenesis. PLoS Genet. *9*, e1003425.

Sartorelli, V., Huang, J., Hamamori, Y., and Kedes, L. (1997). Molecular mechanisms of myogenic coactivation by p300: direct interaction with the activation domain of MyoD and with the MADS box of MEF2C. Mol. Cell. Biol. *17*, 1010–1026.

Sassoon, D., Lyons, G., Wright, W.E., Lin, V., Lassar, A., Weintraub, H., and Buckingham, M. (1989). Expression of two myogenic regulatory factors myogenin and MyoD1 during mouse embryogenesis. Nature *341*, 303–307.

Shi, Y., Lan, F., Matson, C., Mulligan, P., Whetstine, J.R., Cole, P.A., Casero, R.A., and Shi, Y. (2004). Histone demethylation mediated by the nuclear amine oxidase homolog LSD1. Cell *119*, 941–953.

Shi, Y.J., Matson, C., Lan, F., Iwase, S., Baba, T., and Shi, Y. (2005). Regulation of LSD1 histone demethylase activity by its associated factors. Mol. Cell *19*, 857–864.

Tapscott, S.J. (2005). The circuitry of a master switch: Myod and the regulation of skeletal muscle gene transcription. Development *132*, 2685–2695.

Tapscott, S.J., Davis, R.L., Thayer, M.J., Cheng, P.F., Weintraub, H., and Lassar, A.B. (1988). MyoD1: a nuclear phosphoprotein requiring a Myc homology region to convert fibroblasts to myoblasts. Science *242*, 405–411.

Terzi, N., Churchman, L.S., Vasiljeva, L., Weissman, J., and Buratowski, S. (2011). H3K4 trimethylation by Set1 promotes efficient termination by the Nrd1-Nab3-Sen1 pathway. Mol. Cell. Biol. *31*, 3569–3583.

Wang, J., Scully, K., Zhu, X., Cai, L., Zhang, J., Prefontaine, G.G., Krones, A., Ohgi, K.A., Zhu, P., Garcia-Bassets, I., et al. (2007). Opposing LSD1 complexes function in developmental gene activation and repression programmes. Nature *446*, 882–887.

Whyte, W.A., Bilodeau, S., Orlando, D.A., Hoke, H.A., Frampton, G.M., Foster, C.T., Cowley, S.M., and Young, R.A. (2012). Enhancer decommissioning by LSD1 during embryonic stem cell differentiation. Nature *482*, 221–225.

Yang, M., Gocke, C.B., Luo, X., Borek, D., Tomchick, D.R., Machius, M., Otwinowski, Z., and Yu, H. (2006). Structural basis for CoREST-dependent demethylation of nucleosomes by the human LSD1 histone demethylase. Mol. Cell *23*, 377–387.

Yang, J.H., Song, Y., Seol, J.H., Park, J.Y., Yang, Y.J., Han, J.W., Youn, H.D., and Cho, E.J. (2011). Myogenic transcriptional activation of MyoD mediated by replication-independent histone deposition. Proc. Natl. Acad. Sci. USA *108*, 85–90.

Zhu, D., Hölz, S., Metzger, E., Pavlovic, M., Jandausch, A., Jilg, C., Galgoczy, P., Herz, C., Moser, M., Metzger, D., et al. (2014). Lysine-specific demethylase 1 regulates differentiation onset and migration of trophoblast stem cells. Nat. Commun. *5*, 3174.

Zylicz, J.J., Dietmann, S., Günesdogan, U., Hackett, J.A., Cougot, D., Lee, C., and Surani, M.A. (2015). Chromatin dynamics and the role of G9a in gene regulation and enhancer silencing during early mouse development. eLife *4*.

Cell Reports, Volume *18*

Supplemental Information

LSD1 Controls Timely *MyoD* Expression via MyoD Core Enhancer Transcription

Isabella Scionti, Shinichiro Hayashi, Sandrine Mouradian, Emmanuelle Girard, Joana Esteves de Lima, Véronique Morel, Thomas Simonet, Maud Wurmser, Pascal Maire, Katia Ancelin, Eric Metzger, Roland Schüle, Evelyne Goillot, Frederic Relaix, and Laurent Schaeffer

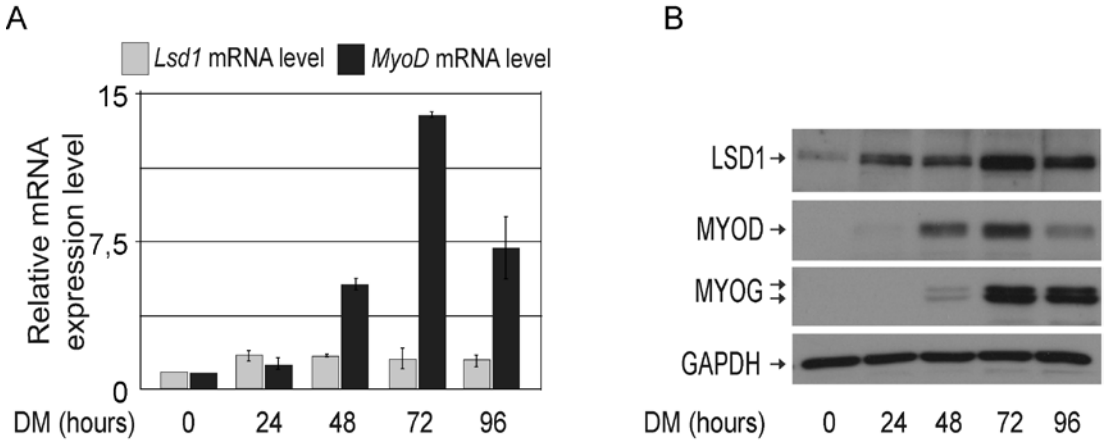

Figure S1. [LSD1 and MyoD expression during C2C12 myoblast differentiation], Related to Figure 1.
A) *Lsd1* and *MyoD* mRNA levels in C2C12 cells during differentiation. RT–qPCR values were normalized to the *Ppib* mRNA levels. mRNA levels are shown as the fold variation compared to C2C12 cells at DM0, i.e., in proliferation conditions. Data are represented as mean ± SEM of at least three experiments. B) LSD1, MYOD and MYOG immunoblots on C2C12 cell extracts during differentiation. GAPDH was used as a loading control.

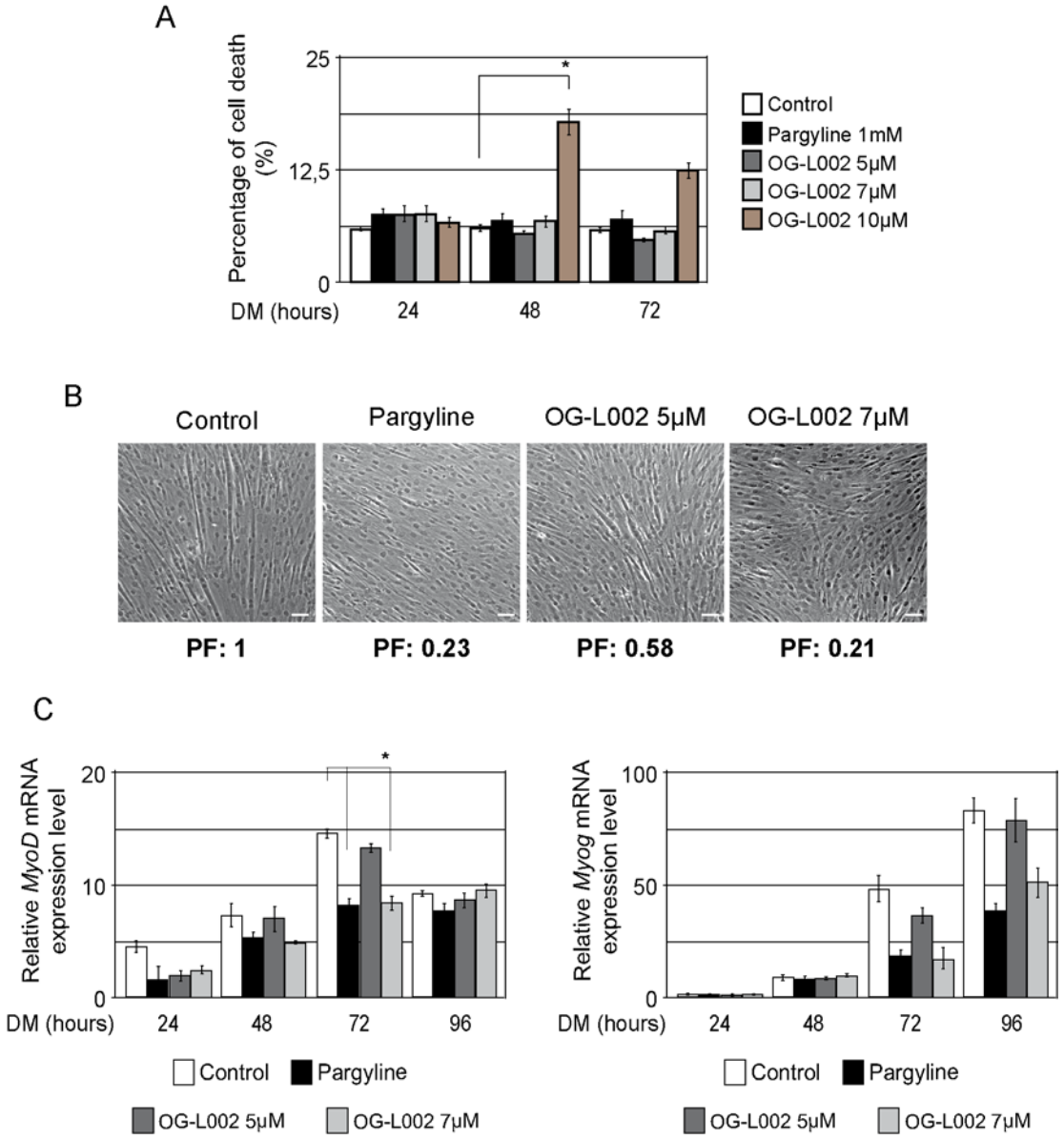

Figure S2. [LSD1 demethylase activity is required to induce myoblast differentiation], Related to Figure 1.
A) Percentage of C2C12 cell death at 24, 48 and 72 hours of differentiation after treatment with Pargyline 1mM and OG-L002 at three different concentrations (5µM, 7µM and 10µM). Measurements were made by cytometry analysis after cell suspension staining with propidium iodide. Data are represented as mean ± SEM of at least three experiments. B) Phase contrast images of Pargyline 1mM and OG-L002 (5µM and 7µM) treated C2C12 cells after 120 hours in DM. Percentage of fusion (PF), calculated as the proportion of cells containing two or more nuclei, are shown below the pictures. Scale bar: 50 µm. C) *MyoD* and *Myog* mRNA levels in C2C12 cells treated with Pargyline 1mM and OG-L002 5µM and 7µM during differentiation. RT–qPCR values were normalized to *Ppib* mRNA levels, and are shown as the fold difference with C2C12 at DM0. Data are represented as mean ± SEM of at least three experiments. *p <0,01 (Bonferroni test after one way ANOVA).

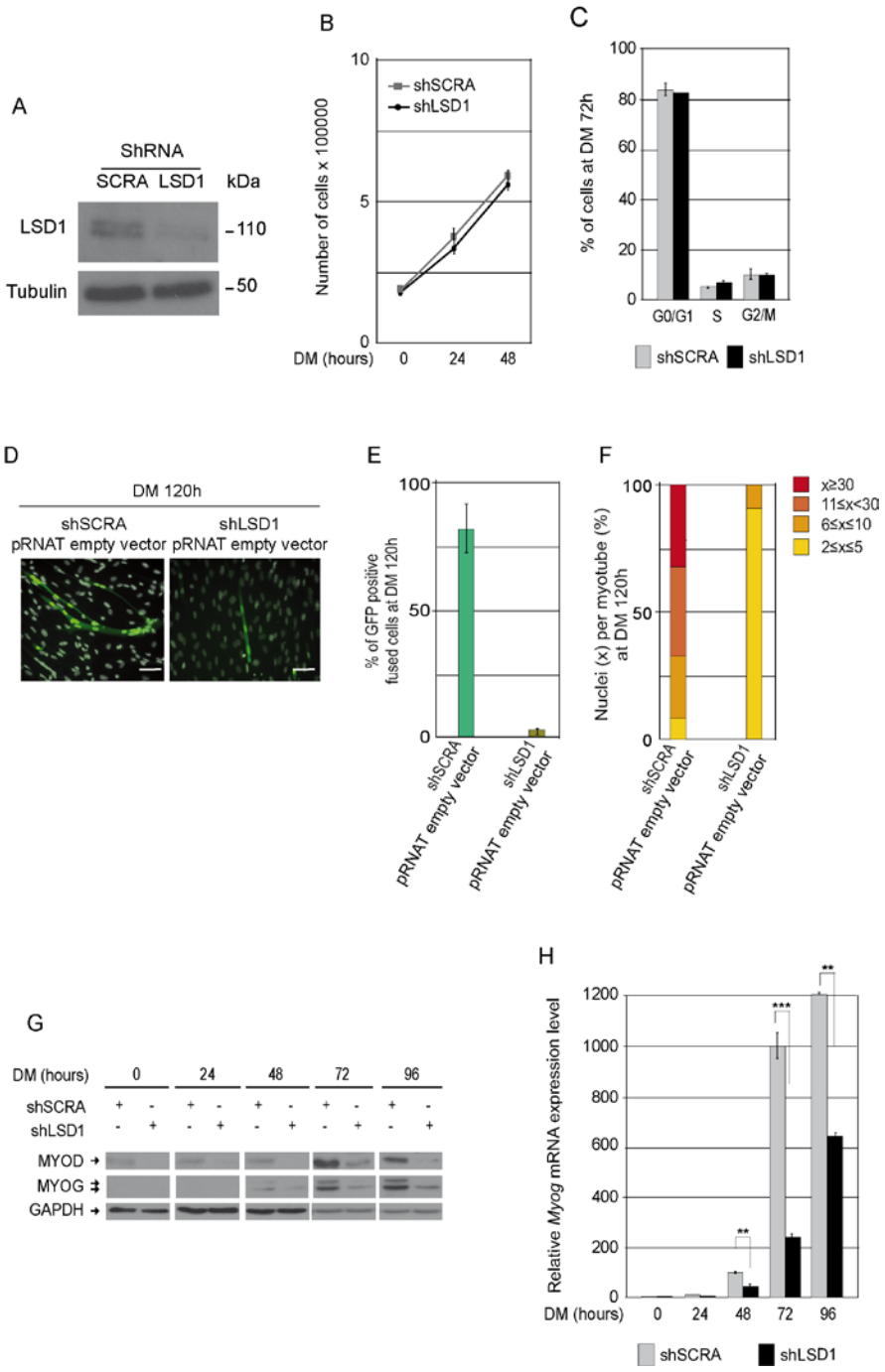

Figure S3. [Absence of LSD1 does not affect myoblast proliferation but impairs their differentiation], Related to Figure 1.

A) Immunoblot for LSD1 on shSCRA and shLSD1 cell extracts showing the efficiency of the shRNA targeting LSD1. Tubulin was used as a loading control. B) shLSD1 and shSCRA cell numbers at DM0, DM 24hours and DM 48 hours. C) shSCRA and shLSD1 cell cycle analysis by cytometry after 72 hours in DM. D) pRNAT vector expressing GFP was transfected in shLSD1 and shSCRA myoblasts to help distinguish cell contours. Cells were allowed to differentiate in DM for 120 hours and were stained with DAPI to visualize nuclei. Transfected cells, identified by green fluorescence, were observed by epifluorescence microscopy. Representative images of GFP positive shLSD1 and shSCRA cells are shown. DAPI was changed to grey to allow better visualization. Scale bars represent 50 µm. E) The percentage of fused cells was calculated as the proportion of GFP positive cells containing two or more nuclei. F) The number of nuclei in 100 shLSD1- and 110 shSCRA- GFP positive cells was counted. G) MYOD and MYOG immunoblots on shSCRA and shLSD1 cell extracts. GAPDH was used as a loading control. H) *Myog* mRNA levels in shSCRA and shLSD1 cells during differentiation. RT–qPCR values were normalized to the *Ppib* mRNA levels, and are shown as the fold difference with shSCRA at DM0. Data are represented as mean ± SEM. **p < 0.01, ***p <0,001 (Bonferroni test after one way ANOVA).

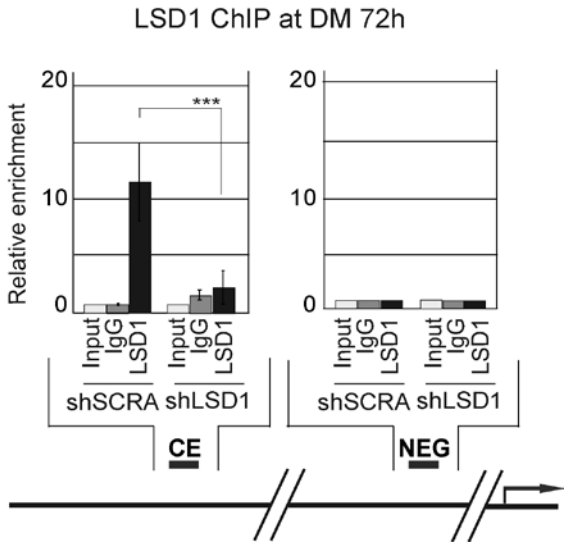

Figure S4. [Validation of LSD1 antibody], Related to Figure 2.
Localization of LSD1 at the Core Enhancer (CE) region of MyoD gene locus after 72 hours in DM. ChIP analysis was performed on shSCRA and shLSD1 cells with an anti-LSD1 antibody. Ct values were normalized to input. Two sites Core enhancer (CE) and Negative regions (NEG) were tested for RT-qPCR amplification. Data are shown as relative enrichment to the NEG region. Data are represented as mean ± SEM of at least three experiments. ***$p < 0.0005$ (Bonferroni test after one way-ANOVA).

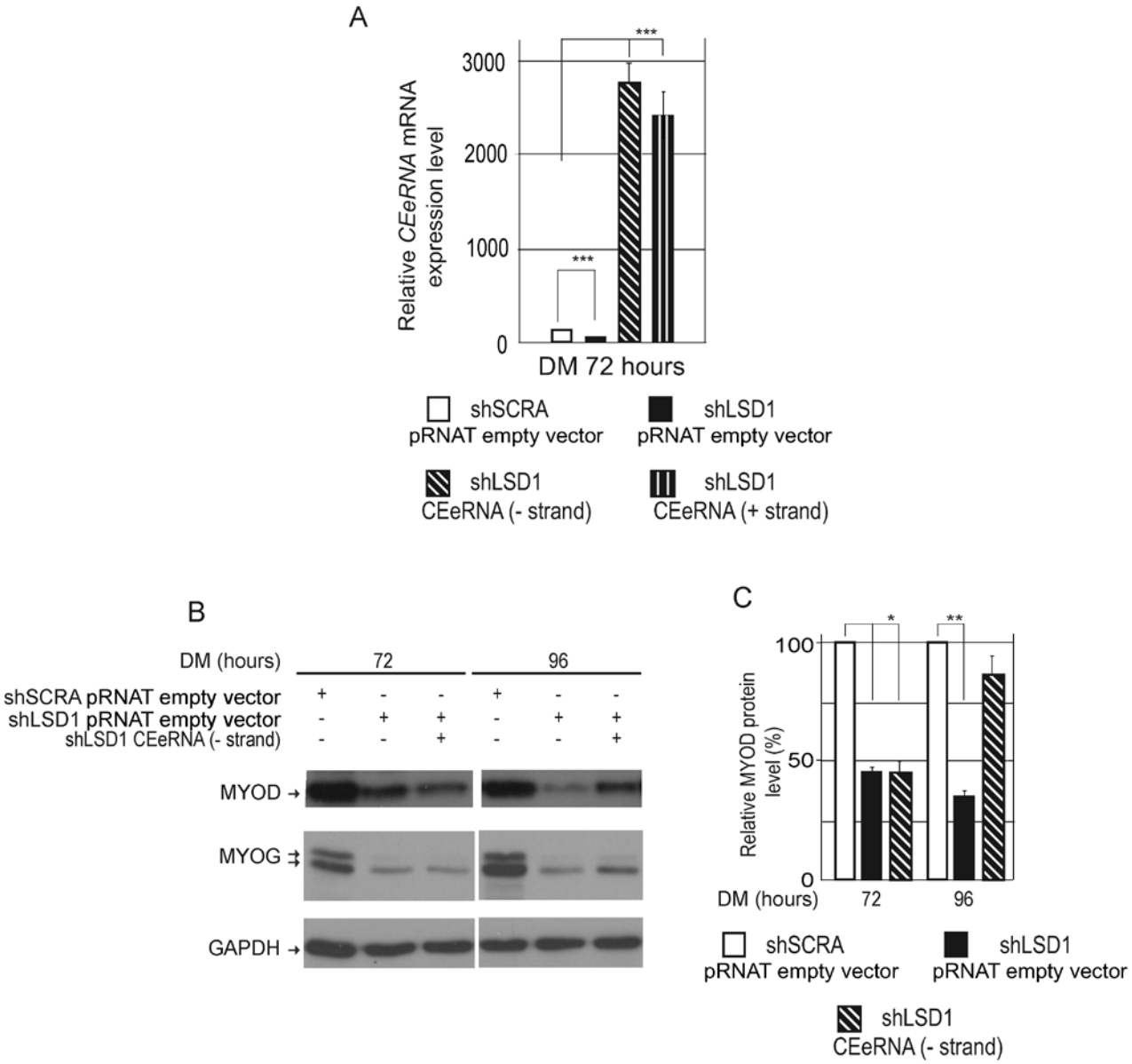

Figure S5. [CEeRNA expression is required for MyoD expression], Related to Figure 4.
A) CEeRNA mRNA levels in shSCRA transiently transfected with pRNAT empty vector, and in shLSD1 cells transiently transfected with empty pRNAT, CEeRNA (- strand) or CEeRNA (+ strand) vectors after 72 hours in DM. RT–qPCR values were normalized to *Ppib* mRNA levels and are shown as the fold difference with shSCRA at DM0. B) MYOD and MYOG immunoblots on extracts of shSCRA cells transiently transfected with empty pRNAT vector and shLSD1 cells transiently transfected with empty pRNAT or CEeRNA (- strand) vectors after 72 and 96 hours in DM. GAPDH was used as loading control. C) Relative MYOD protein levels were quantified using Image J software and compared to MYOD in shSCRA control cells. Data are represented as mean ± SEM of at least three experiments. *$p < 0.05$, **$p < 0.01$. ***$p < 0.005$ (Bonferroni test after one way ANOVA).

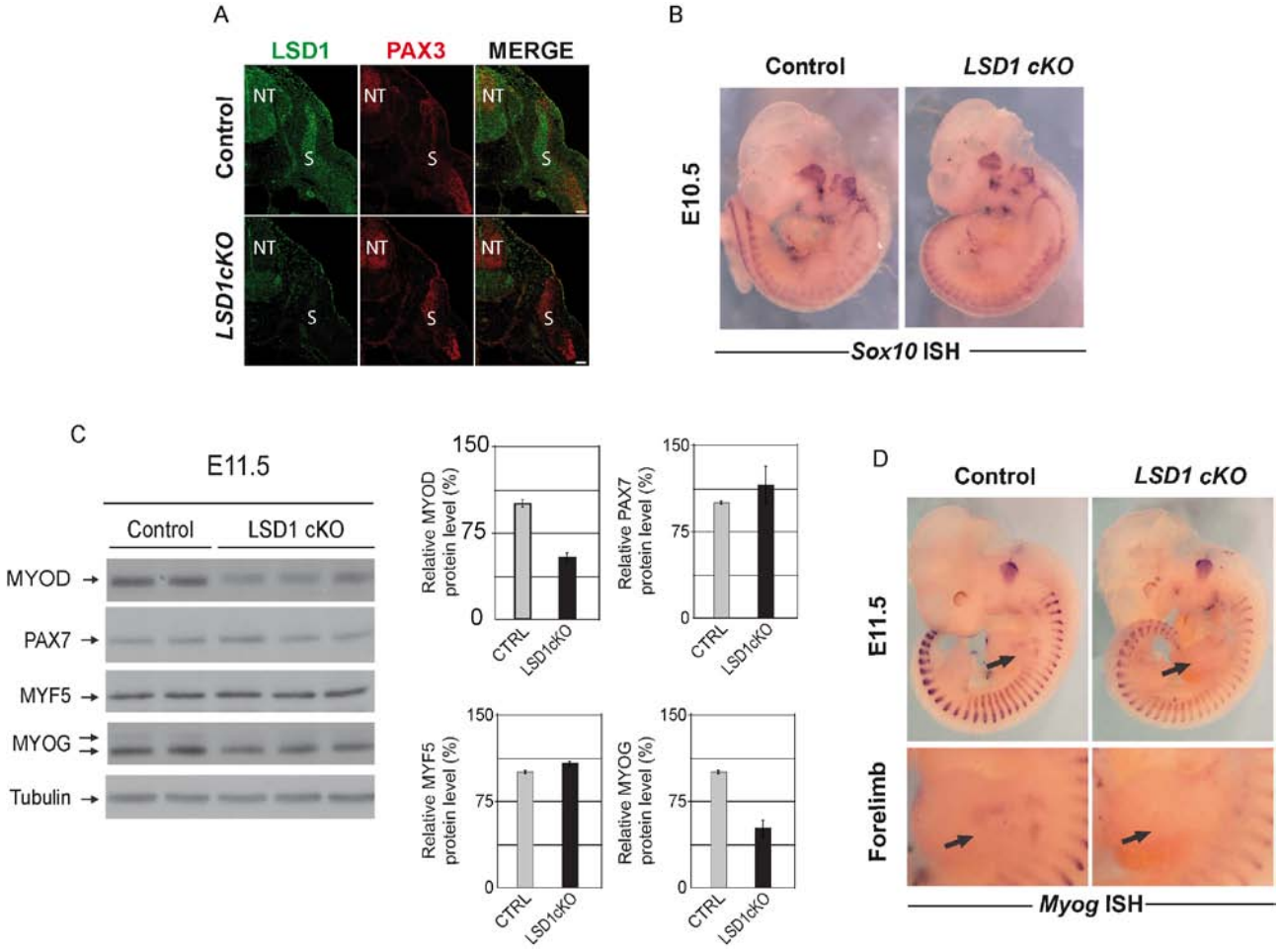

Figure S6. [LSD1 deficiency does not affect peripheral nervous system development but delayed myogenesis in vivo], Related to Figure 6.

A) LSD1 and PAX3 immunostainings of transverse sections of E11.5 control and LSD1cKO embryos in the neural tube (NT) and the somites (S). Scale bars represent 50 µm. B) Whole-mount *in situ* hybridization with a *Sox10* RNA probe in control and LSD1 cKO embryos at E10.5. C) MYOD, PAX7, MYF5 and MYOG protein levels were analyzed by immunoblotting E11.5 control (n=2) and LSD1cKO (n=3) total embryo protein extracts. Relative protein levels were quantified using Image J software and compared to levels in control embryos. D) Whole-mount *in situ* hybridization with *Myog* probe in control and LSD1 cKO embryos at E11.5. Arrowheads show forelimbs. Close-up of the forelimb region (lower panels).

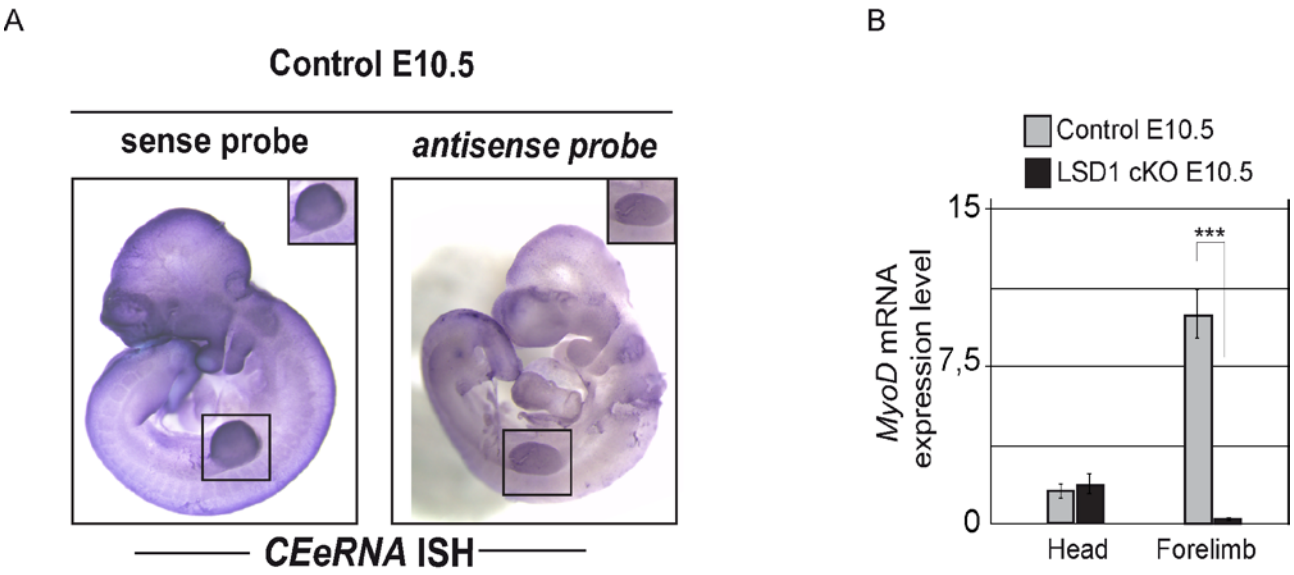

Figure S7. [CEeRNA (– strand) expression in control and LSD1cKO E10.5 embryos], Related to Figure 7.
A)Whole-mount *in situ* hybridization with two CEeRNA RNA probes in E10.5 control embryos. Antisense probe hybridizes the CEeRNA (+ strand) while the sense probe binds the CEeRNA (– strand). Insets are higher magnification of the forelimb region. B) *MyoD* mRNA levels in dissected forelimbs and heads from control (n=6) and LSD1cKO (n=4) embryos at E10.5. RT–qPCR values were normalized to the *Ppib* mRNA levels. Data are represented as mean ± SEM. ***$p < 0.005$ (Bonferroni test after one way ANOVA).

Supplemental Experimental procedures

List of oligonucleotides

Gene or region	Application	Sense primer	Antisense primer
MyoD	RT-qPCR	AGCACTACAGTGGCGACTCA	GCTCCACTATGCTGGACAGG
Ppib	RT-qPCR	GATGGCACAGGAGGAAAGAG	AACTTTGCCGAAAACCACAT
CEeRNA	RT-qPCR	GCCAAGTATCCTCCTCCAGC	AAGCTGAGCACTCTGGGAGA
Myog	RT-qPCR	CAATGCACTGGAGTTCGGTC	ACAATCTCAGTTGGGCATGG
MyoD TSS	ChIP	AGATAGCCAAGTGCTACCGC	CCAGGGTAGCCTAAAAGCCC
MyoD NEG	ChIP	CCCTTCATCCAGGGCACTAC	TTGGGAACCCAGCAGTAAGC
MyoD CE	ChIP	CTAAACACCAGGCATGAGAGG	ACTCACTTTCTCCCAGAGTTGC
CEeRNA	Cloning	CACGTGATGAAAAGTGAGGACA	TGACGTCACCAACAACGGTA
CEeRNA	ISH	GGAGCACCCCACAACATGAGC	AGTCTGTGCGGGTGAGGCAG

List of antibodies

Name	Application	Compagny
Anti-LSD1	ChIP 5µg/IP IF 1:100	Abcam
Anti-LSD1	Western blotting 1:1000	Active motif®
Anti-MYOD	Western blotting 1:500 IF 1:200	Santa-cruz Biotecnology®
Anti-MYOG	Western blotting 1:200	Santa-cruz Biotecnology®
Anti-GAPDH	Western blotting 1:10000	Cell signaling technology®
Anti-H3K4me1	ChIP 5µg/IP	MilliporeTM
Anti-H3K4me3	ChIP 5µg/IP	MilliporeTM
Anti-H3K9me2	ChIP 5µg/IP	Active motif®
Anti-H3K9me3	ChIP 5µg/IP	MilliporeTM
Anti-H3	ChIP 5µg/IP	Active motif®
Anti-MYF5	Western blotting 1:500	Santa-cruz Biotecnology®
Anti-PAX3	IF 1:100	DSHB
Anti-PAX7	Western blotting 1:200	Santa-cruz Biotecnology®
Anti-RNApol II	ChIP 5µg/IP	Abcam
Anti-α Tubulin	Western blotting 1:20000	Sigma